GFZ

Helmholtz-Zentrum
POTSDAM

Originally published as:

Manuscript accepted for publication in Computers and Geoscience

Influence of dike breaches on flood frequency estimation

Apel, H.[a], Merz, B.[a], Thieken, A.H.[a]

[a] GeoForschungsZentrum Potsdam (GFZ)

Telegrafenberg

14473 Potsdam

Germany

hapel@gfz-potsdam.de, bmerz@gfz-potsdam.de, thieken@gfz-potsdam.de

corresponding author:

Heiko Apel

Tel.: +49 331 288 1538

Fax: +49 331 288 1570

E-mail: hapel@gfz-potsdam.de

Abstract

Many river floodplains and their assets are protected by dikes. In case of extreme flood events, dikes may breach and flood water may spill over into the dike hinterland. Depending on the specific situation, e.g. time and location of breach, and the capacity of the hinterland to contain the flood water, dike breaches may lead to significant reductions of flood peaks downstream of breach locations. However, the influence of dike breaches on flood frequency distributions along rivers has not been systematically analysed. In order to quantify this

influence a dynamic-probabilistic model is developed. This model combines simplified flood process modules in a Monte Carlo framework. The simplifications allows for the simulation of a large number of different scenarios, taking into account the main physical processes. By using a Monte Carlo approach, frequency distributions can be derived from the simulations. In this way, process understanding and the characteristics of the river-dike-floodplain system are included in the derivation of flood frequency statements. The dynamic-probabilistic model is applied to the Lower Rhine in Germany and compared to the usually used flood frequency analysis. For extreme floods the model simulates significant retention effects due to dike breaches, which lead to significant modifications of the flood frequency curve downstream of breach locations. The resulting probabilistic statements are much more realistic than those of the flood frequency approach, since the dynamic-probabilistic model incorporates an important flood process, i.e. dike breaching, that only occurs when a certain threshold is reached. Beyond this point the behaviour of the flood frequency curve is dominated by this process.

Keywords: flood frequency, dike breach, floodplain retention, probabilistic dynamic modelling

1. Introduction

The sound estimation of flood hazards is of particular relevance along large rivers where usually high damage potential has been accumulated over time, e.g. due to growth of urban areas or industrial sites. In many cases these areas are protected by river dikes. However, extraordinary floods may cause dike breaches and consequently high damages. For example, during the August 2002 floods more than 130 dike breaches occurred in Germany along the Elbe and its tributaries causing a total damage of approximately 15 billion €

Depending on the characteristics of the river, the floodplains, the dikes and the characteristics of the dike breach, such as location and width of the breach, significant volumes of water may spill over into the dike hinterland, reducing the peak of the flood wave downstream of the breach location. This effect has been observed in the course of actual flood events (e.g. Engel, 2004), and it has been simulated for synthetic situations (e.g. Kamrath et al., 2006). Also the attenuation effect of flood plains has been studied in reaches without flood protection (Jothityangkoon and Sivapalan, 2003; Woltemade and Potter, 1994). However, the influence of dike breaches on the flood hazard situation along rivers has not been investigated systematically. This paper investigates particular influence for the Lower Rhine in Germany.

Flood hazard assessment is an essential basis for the development of flood mitigation schemes. Flood hazard is traditionally defined as the exceedance probability of potentially damaging flood situations in a given area and within a specified period of time. Flood hazard assessments for river reaches are usually based on a number of flood scenarios. Each scenario is associated with a certain exceedance probability P_E or return period T. For example, in many countries, such as United Kingdom, Germany, Italy, Spain, France, USA, Canada and New Zealand, the area affected by a 100-year flood plays an essential role for flood mitigation strategies. The proposed directive of the European Union on the assessment and management of floods requires two flood scenarios with return periods of 10 and 100 years, respectively, and an extreme scenario with a higher return period (EU, 2006). The same choice was made

3

by the International Commission for the Protection of the Rhine: The Rhine-Atlas with a scale of 1:100000 provides an overview of the flood situation for the 10-year, the 100-year and an extreme event (ICPR, 2001).

Such flood hazard assessments consist of two steps: (1) estimating the T-year discharge along the watercourse, and (2) transferring the discharge values into inundation areas. The most widespread approach for the estimation of the T-year discharge along rivers is flood frequency analysis, i.e. the application of extreme value statistics to a record of observed discharges at the locations of interest (e.g. Stedinger et al., 1993). In many cases, at-site (local) frequency analysis is complemented by regional flood frequency analysis, using data from gauging stations that are supposed to have similar flood behaviour (e.g. Hosking and Wallis, 1997).

Flood frequency analysis suffers from various drawbacks, originating from insufficient data sets, and possible violation of the underlying assumptions of extreme value statistics. Discharge data series are hardly longer than 30-50 years. Consequently, an estimation of floods with return periods above 100 years is a wide extrapolation and hence highly uncertain. In those rare cases where longer time series exist, earlier periods might not be representative for today's situation, and the basic assumptions of extreme value statistics, namely stationarity and homogeneity, might be violated.

Stationarity requires that the flood runoff randomly fluctuates in time with a constant pattern around a constant mean value. This implies that flood producing processes, e.g. rainfall regime or geomorphological characteristics of the catchment, do not change with time. Several studies have challenged the assumption of stationarity in flood frequency analysis due to climate variability (e.g. Jain and Lall, 2001; Milly et al., 2002; Pfister et al., 2004, Kingston et al., 2006) or human impact on hydrological processes (Helms et al., 2002, Lammerson et al., 2002, Pfister et al., 2004).

4

The assumption of homogeneity is violated if floods in the observation range and in the extrapolation range are caused or significantly influenced by different processes. Gutknecht (1994) discusses flood generation in small mountainous catchments and suggests that extreme flood events are caused by other meteorological, hydrological, hydraulic or geomorphological processes than frequent floods. The assumption of homogeneity may not hold either for floods that overtop and breach river dikes. Dike breaches might not have occurred during the observation period. Therefore, in the extrapolation range an additional process, namely retention of flood water due to dike breaches, appears that is not contained in the observed data set. Even if dike breaches had occurred in the observation period, the flood defence system would have been redesigned, possibly leading to significant changes in the river-flood system.

The simplest method for the second step of a flood hazard assessment, i.e. the transfer of discharge values in flooded areas, is based on the rating curves at the gauges and the floodplain DEM (Digital Elevation Model). The discharges for selected return periods T are converted to water levels via the rating curve. Further, the water levels between gauging stations are interpolated, and the T-year flooded area is obtained by intersecting the interpolated water level with the DTM. This simple method does not consider dike breaches. In some cases, it is applied to the situation with and without dikes, thus giving a rough idea of the flood defence effects of dikes. In flat lowland areas the intersection of DEM and water level at the gauge might produce unrealistic inundation extends, because the inundation area might be limited by the water volume available for flooding, an effect that is not considered by the intersection of water level and DEM.

More sophisticated methods use 1D or 2D hydrodynamic models to simulate the flooded area associated with a certain discharge value. Such approaches can include the effects of dike breaches. However, since the T-year discharge for certain river sections is taken from the

flood frequency analysis, the effects of upstream dike breaches do not propagate, and they do not affect the flood frequency analysis at downstream gauges.

Besides the approaches that build on flood frequency analysis, deterministic, scenario-based approaches are used to investigate the effects of dike breaches (e.g. Alkema and Middlekoop, 2005, Kamrath et al., 2006). These approaches are based on simulation models that describe the processes of flood routing in the river (usually 1D hydrodynamic model), dike breaching and flooding of the hinterland (usually 2D hydrodynamic model). They are able to consider the downstream effects of dike breaches. However, since they only consider deterministic scenarios, it is not clear how this information can be incorporated into flood frequency statements. Further, they are computationally very demanding, which limits the possibility of simulating many scenarios.

The aim of this paper is to investigate how flood frequency distributions along river reaches are influenced by dike breaches. We start from the hypothesis that, under extreme hydrological loading, river dike breaches might significantly influence the shape of the flood frequency distribution. To this end, we extend a dynamic-probabilistic model that has been developed and applied to the Lower Rhine by Apel et al. (2004, 2006). This approach combines simplified flood process models in a Monte Carlo framework. The simplifications allow us to simulate a large number of different scenarios, taking into account the main physical processes. By using a Monte Carlo approach, frequency distributions can be derived from the simulations. The model results are compared to the usual approach for flood hazard assessment along rivers.

2. Study area

The investigation area in this study is a reach of the Lower Rhine in Germany between gauge Cologne (Rhine-km 688) and gauge Rees (Rhine-km 837) near the German-Dutch border

(Figure 1). The two major tributaries within the reach are the rivers Ruhr and Lippe. Their input to the system is considered in the modelling approach.

The stretch of the river represents a typical large lowland river with wide meanders and is almost completely protected by dikes on both sides. The total length of the embankments at the Lower Rhine amounts to 330 km and the safety levels vary between a 20-year flood for small summer dikes and a 500-year flood for the main structures (ICPR, 2001). The hinterland behind the dikes has a large damage potential due to many densely populated settlements and industrial areas. Assuming an extreme event (i.e. approximately a 500-year flood) the ICRP (2001) estimates an area of 1356 km² at risk of inundation along the Lower Rhine with a direct economic losses of 20333 million Euro. However, according to MURL (2000) the inundated area is reduced to 420 km² by the embankments.

All the dikes in the reach were rebuilt in the last decades according to the engineering state of the art. They are zonated dikes with an impermeable surface layer at the water side connected to an impermeable basement, and a draining permeable layer at the land side often accompanied with a basement drainage. This construction type minimises the probability of dike failure due to piping, i.e. internal erosion, seepage or basement failures.

The flow regime of the River Rhine is dominated by snowmelt and precipitation runoff from the Alps in the summer months, and further downstream by precipitation runoff from the uplands of central Germany and neighbouring countries in winter (Disse and Engel, 2001). The mean daily discharge amounts to 2087 m³/s at gauge Cologne (data from 1880 to 2004) and to 2284 m³/s at gauge Rees (data from 1930 to 2000). Little seasonal variation enables year-round navigability (Disse and Engel, 2001).

At the Lower Rhine, floods frequently occur during winter and early spring. In the annual maximum discharge series from 1880 to 2004 only 7 % of the annual maxima (9 events) at the gauge Cologne occurred in summer (May – September) whereas 85 % took place between November and March.

Severe flood events occurred in December 1993 and January 1995. Both events originated in the uplands of the Middle and Lower Rhine where heavy precipitation fell on saturated or frozen soil resulting in high runoff coefficients (see Chbab, 1995, Fink et al., 1996). In Cologne, the maximum water levels amounted to 10.61 m (~ 10700 m³/s) in 1993 and 10.69 m (~ 10800 m³/s) in 1995. In 1995, a damage of 33.23 million Euro occurred in Cologne and was only about half of that associated to the 1993 flood (Fink et al., 1996). This effect was also observed in other municipalities and was mainly attributed to improved preparedness and disaster management (Wind et al., 1999).

3. Dynamic-probabilistic approach for flood hazard assessment

3.1 Outline of the approach

The dynamic-probabilistic approach is a set of modules, each representing a component in the flood processes of the study area:

- Hydrological input at Cologne:

  At gauge Cologne, the upstream boundary of the system, the input into the system in terms of flood peak and shape of flood hydrograph is described.

- Superposition of flood waves of Rhine and of major tributaries:

  The behaviour of the main tributaries Lippe and Ruhr is of importance for the flood situation in the Lower Rhine. High flood peaks of Lippe and Ruhr at times of high discharge values in the Rhine aggravates the flood situation of the Lower Rhine. Therefore, the interplay of flood peaks and hydrograph shape between the Rhine and the tributaries is taken into account.

- Hydraulic transformation:

  This module calculates water levels in the river reach for given discharges.

- Dike failure due to overtopping and outflow through dike breach:

This module tests whether dike segments are overtopped. In this case, a two-dimensional dike fragility curve is applied which estimates the probability of a dike breach under a given hydrological load. If a breach occurs, a breach width is selected and the outflow into the hinterland is determined, which corresponds to a decrease in flood volume downstream of the breach location.

For each of these processes simple and computationally efficient models were developed. They are based on several pre-processing works. With the exception of the module 'Hydraulic transformation', all modules contain probabilistic elements. This approach reflects the inherent variability of flood processes and our inability to deterministically describe such processes as the superposition of flood peaks of the Rhine and its tributaries. The modules are linked and embedded in a Monte-Carlo simulation framework. Each Monte-Carlo run generates a single flood event resulting in an ensemble of flood events from which empirical probabilities can be derived.

The following sections give a short description of the modules. A more detailed description can be found in Apel et al. (2004, 2006). The module 'dike failure due to overtopping and outflow through dike breach' is described in detail, since this module was extended to account for a quasi-continuous mode of dike failure along the complete study area. The model version of Apel et al. (2004, 2006) was restricted to two dike breach locations only.

3.2 Hydrological input at Cologne

For each flood event that is generated by the modelling system we need the input into the river system at its upstream boundary, i.e. at the gauge Cologne/Rhine. Since the retention effects of dike breaches are studied, the complete hydrograph at gauge Cologne has to be generated for each event. This procedure is divided into two steps. In the first step a flood peak value is generated, and in the second step a hydrograph is assigned to this peak value.

The flood peaks are estimated by means of a flood frequency analysis, based on the observation data at gauge Cologne. It is well known that the choice of the distribution function may significantly influence the result of flood frequency analysis. Different types of distribution functions can be applied, usually leading to very different flood quantiles in the extrapolation range. From the spectrum of distribution functions used in flood frequency analysis, the following set of functions representative for the different classes of eytreme value distribution functions was chosen: Gumbel, LogNormal, Weibull, Pearson III and Generalized Extreme Value (GEV), (Stedinger et al., 1993). This subjective selection was performed under the assumption of no a priori knowledge of the most appropriate function type for the region and with the intention to cover the functions frequently used as well as all classes of distribution function types.

The functions are fitted to the data sets by the method of moments, except for the GEV where L-moments are used. The goodness of fit of the different functions is assessed by a maximum likelihood method (Wood and Rodriguez-Iturbe, 1975). Based on this fitting criterion, a composite distribution function is derived by weighing the different distribution functions according to Wood and Rodriguez-Iturbe (1975). Figure 2 shows the fitted distribution functions to the data set of Cologne along with the maximum likelihood weights.

The annual maximum discharge series of the gauge Cologne for the period 1961-1995 is used, although much longer series exist. Extensive river training works and retention measures, the construction of weirs along the Upper Rhine, and effects of climate variability suggest significant changes in the flood behaviour during the first half of the 20th century (Lammersen et al., 2002, Pfister et al., 2004). Therefore, former observations might not be representative for the current state of the river system.

To obtain hydrographs, typical normalised hydrographs are extracted from the discharge data series: For every year the maximum flood event was extracted from the hourly discharge series and normalised to flood peak discharge and time to peak discharge. The resulting 35

normalised flood hydrographs were subjected to a cluster analysis yielding seven characteristic flood waves (i.e. seven clusters). The clusters can be grouped into short single peaked, short waves with small peaks preceding maximum and long multiple peaked flood events (Apel et al., 2004). The normalised hydrographs are assumed to be independent from the return periods. However, each normalised flood waves is assigned with an occurrence probability, which is equal to the proportion of the number of flood events in the respective cluster to the total 35 flood events, thus indicating the probability of the annual maximum flood to belong to a single cluster. These occurrence probabilities are not to be confused with return periods of flood peak discharge.

3.3 Superposition of flood waves of Rhine and tributaries

The interplay between floods in the main river and floods in the tributaries is considered by a correlation analysis of the annual maximum discharges of the main river and the corresponding events in the tributaries. The analysis shows that a rather tight linear correlation between the discharge peaks of the Rhine and the peaks of Lippe and Ruhr exist. This correlation in combination with the confidence intervals of the linear regression is used to randomly generate a peak value for the tributaries, given the peak value of the Rhine (Apel et al., 2004).

For each hydrograph cluster of the Rhine, the corresponding mean shapes of the hydrographs of the tributaries are derived, based on the annual maximum data of gauges Hattingen/Ruhr and Schermbeck I/Lippe for the period 1961-1995. In the Monte-Carlo simulation for each generated flood event the mean hydrograph of the same cluster as the main river is chosen at the tributaries, thus retaining the dependency of the flood events in main river and tributaries. This dependency is caused by similar flood generating processes, i.e. high precipitation events in the uplands of the Middle and Lower Rhine (cf. section study area). Figure 3 shows the superposition of the synthetic main and tributary flood events for all seven flood types. It can

be seen that the flood waves of main river and tributaries show similar characteristics in all clusters thus indicating the identical generating processes mentioned above. However, the peaks do not overlay. In some cases the tributaries precede the peak in the main river, in others they follow. This can be interpreted as a result of different cyclone pathways causing the different precipitation fields in the uplands.

3.4 Flood routing and hydraulic transformation

1D-hydrodynamic simulations of flows in the investigated reach have shown that the flood peak attenuation and the stretching of the flood wave in the reach are negligible. Figure 4 shows the flood wave of the flood of December 1993, which is hardly modified within the 160 km under study. The increase in the flood peak flow can be attributed to the tributary inputs, even for the subreach between Cologne and Düsseldorf, where minor tributaries join the Rhine. This results in an increase in flood peak flow of 72 m^3/s in the subreach, which is equivalent to an increase in stage of 3 cm at gauge Düsseldorf. This minor flood peak deformation, which is below the accuracy of the digital elevation model and the surveyed dike elevations, can be assumed for the complete reach, because no major changes in the river morphology occur further downstream. Therefore the routing effect is neglected in this study, which reduces the computational effort considerably.

However, in order to obtain discharge-stage curves for every breach location (cf. section 3.5) the 1D-hydrodynamic model HEC-RAS (Brunner, 2002) with cross sections every 500 m was adapted to the Lower Rhine. Using a simulation of the flood event of 1995, the discharge-stage curves were extracted from the simulation results at the appropriate cross sections.

3.5 Dike failure due to overtopping and outflow through dike breach

Breach locations

This module tests whether dikes are overtopped and possibly breach for a given flood wave. In case of breaching, it calculates the outflow in the hinterland and the reduction of the flood wave in the main river.

Almost the complete river reach in the study area is accompanied by dikes, i.e. there are almost 330 km of dikes. In principle, a dike breach could occur at each point along the dike lines. A continuous test for dike breaching would require an enormous amount of CPU-time, especially in a Monte-Carlo framework. Therefore, a quasi-continuous scheme was developed which is supposed to reduce the potential dike breaching locations to a manageable number. The scheme is comprised of the following steps:

1. 2D-inundation simulations are performed every kilometre on both sides of the river for a fixed breach width of 100 m and a breach depth reaching the basement of the dike. A constant breach outflow is assumed approximating the outflow in case of river water levels at dike crest height. The breach outflow is calculated with a standard formula for broad crested weirs.

2. The inundated areas of the breaches at different locations are compared and grouped according to the similarity of the inundation areas. Each of these groups represents a model breach location, where the model breach is located in the midpoint of the dike section of the group.

By this procedure 41 model breach locations were identified on both sides of the river along the complete reach (Figure 1). For the 2D-inundation simulations, a raster model based on the diffusion wave analogy, an approximation of the full St.-Venant equations, was used. The approach is identically to the floodplain inundation part of LISFLOOD-FP developed by Bates and De Roo (2000). The simulations were performed on the basis of a Digital Elevation Model with grid size of 50 m using the adaptive time-stepping given by Hunter et al. (2005). The roughness parameterisation was derived on the basis of the CORINE land use data with

parameters assigned to each land use class according to published values (Werner et al., 2005; Chow, 1973).

Dike failure mechanism and probability

Dikes may breach due to different failure mechanisms, such as erosion of the dike surface due to overtopping, instability due to seepage or piping of the dike itself or of its underground, and sliding of the dike. The analysis in this paper is restricted to the mechanism 'breach as consequence of overtopping'. The dikes in the study area are modern 3-zone-dikes and well maintained. According to the authorities responsible for dike safety, the only probable mechanism of dike breaching is due to overtopping. This assumption is supported by the fact that there has been no dike failure at this reach during the last decades, although there have been severe floods with water levels close to the dike crest.

For each model breach location, a fragility surface (or 2D fragility curve) was derived. This surface represents the probability of a breach occurring at certain dike locations as a consequence of overtopping. The failure probability is conditioned on the duration and height of the flood wave overtopping the dike crest. This methodology is an extension of the 1D-fragility curve method described in USACE (1999) and Dawson et al. (2005), which take only one dimension, i.e. the height of the flood wave into account.

The fragility surface results from the comparison of the erosional stress inflicted on the dike surface by the overtopping flood wave and the resistance of the dike. The stress is described by the actual discharge q_a overtopping the dike. The calculation of q_a is performed with a broad crested weir formula especially modified for dike overflow (Kortenhaus and Oumeraci, 2002). The calculation of the resistance q_{crit} follows the approach of Vrijling (2000) and is based on data published in Hewlett et al. (1987). Following these considerations the dike breaches, if $q_a > q_{crit}$ with

$$q_a = A \cdot dh^{3/2} \qquad \text{(Kortenhaus and Oumeraci, 2002)} \qquad (1)$$

$$q_{crit} = \frac{v_c{}^{5/2} \cdot k^{1/4}}{125 \tan \alpha_i{}^{3/4}} \qquad \text{(Vrijling, 2000)} \qquad (2)$$

and

$$v_c = \frac{(3.9117 + 1.5 \cdot (f_g - 1))}{1 + (0.8575 - 0.45 \cdot (fg - 1)) \cdot \log_{10}(t_e)} \qquad (3)$$

where A [m²/s] is a summary parameter representing the geometric features of the dike (see Kortenhaus and Oumeraci, 2002 for details), dh [m] is the difference between the water level and the levee crest, v_c [m/s] is the critical flow velocity, α_i [deg] the angle of the inner talus, k [m] the roughness of the inner talus, f_g [ ] a parameter describing the quality of the turf covering the dike, and t_e the overflow duration [h]. Formula (3) is parameterised on the basis of experimental data given in Hewlett et al. (1987), with $f_g = 1$ representing average turf conditions, $f_g = 0.5$ poor and $f_g = 1.5$ good turf conditions. Figure 5 shows the fit of (3) to the data.

If we had perfect knowledge of the parameters that influence the erosional stress and the dike's resistance, the comparison of q_a with q_{crit} would decide whether the dike breaches or not. Since dike parameters are time- and space-variable and not perfectly known, they are described by probability distribution functions, based on data given by Vrijling (2000) for Dutch river dikes. For a certain dike breach location, the probability of breaching $P(B \mid (dh, t_e))$ for a given couple of overtopping height dh and overtopping duration t_e is calculated by randomly generating dike parameters from the respective distributions (10^4 samples in this study) and evaluating the quantity $q_a - q_{crit}$. $P(B \mid (dh, t_e))$ equals to the relative frequency of failures. This procedure is repeated for the complete domain of dh and t_e, and for three distinct values of f_g (0.5, 1, and 1.5). In this way fragility surfaces for each dike breach location were constructed as exemplarily shown in Figure 6.

During each run of the dynamic-probabilistic model each breach location is tested for failure in downstream order. Given the current combination of *dh* and t_e, the fragility surface yields the probability of failure. In our calculation we assumed an average quality of the turf surface, i.e. $f_g = 1$, for all breach locations.

Breach width

The width of dike breaches strongly influences the spill-over of water into the hinterland. The breach width depends on the actual flow situation during the breach, and on the construction material and geometric properties of the dike. Since there is not enough information to quantify the relation between breach width, dike properties and flow situation, the breach width is assumed as a random variable. Its distribution is based on an evaluation of historical dike breaches at the Rhine in 1882-1883 (Merz et al., 2004). This data set comprises 14 breaches, with a mean breach width of 70.3 m and a standard deviation of 31.5 m. We further assumed a normal distribution of the breach widths. However, we constrained the randomised breach widths to a lower bound equalling the smallest observed breach width of 34 m and an upper bound of 200 m in order to keep the randomised breach widths within a reasonable range.

3.6 Monte Carlo simulation

The four modules are linked in a Monte Carlo simulation. Figure 7 shows the outline of this procedure. Each Monte Carlo run is equally likely and comprises the:

- generation of a flood wave at Cologne,
- generation of tributary flood waves, conditioned on the flood wave in the main river,
- transformation of discharges into stages at each model breach location,
- test for overtopping at each model breach location,
- in case of overtopping: calculation of the breach probability conditioned on the actual overtopping height and duration using the fragility surfaces, and random

determination of breaching (based on the calculated breach probability and a randomly drawn number),

- in case of breaching: generation of breach width,

- in case of breaching: calculation of flow into the hinterland and reduction of the flood wave in the main river,

- superposition of the tributary flood waves at the appropriate routing nodes.

This procedure is repeated 10^5 times, yielding 10^5 synthetic flood events. In empirical tests this number of Monte Carlo runs proved to yield stable results up to return intervals of 10^4 years. Since the event generation is based on annual maximum discharge data, the resulting discharge and damage series are considered as annual maximum series. Thus annual exceedance probabilities and return periods can be derived from the generated data sets.

4. Results

In 150 of 10^5 model runs dike breaches occurred. All breaches were concentrated at the first six model breach locations, i.e. at the upstream end of the river system. The hinterland of these dike segments can contain large flood volumes. Therefore, these breaches reduce the flood waves even in an extreme event such that further downstream the dikes are not overtopped and hence the considered breach mechanism is not triggered. The retention effect due to dike breaching is thus well reproduced by the model system.

Figure 8 shows the effect of the dike breaches on the discharges associated to events with selected return intervals along the river reach. For the gauging stations downstream of Cologne (Düsseldorf, Ruhrort, Rees) the dynamic-probabilistic model yields lower discharges for rare events in comparison to the flood frequency analysis. described in section 3. The reduction is particularly dramatic for the 5000-year flood. The lower discharge values for large events is a consequence of the dike breaches and the flood attenuating effect of the

inundation of the hinterland. For lower return intervals (100, 200, 500 years) the dynamic-probabilistic model yields slightly larger discharges than the flood frequency analysis, which results from the different shapes of the distribution function of the downstream gauging stations in comparison to Cologne.

These effects are also illustrated in Figure 9 showing the flood frequency curves for Düsseldorf, Ruhrort and Rees. For each station the frequency analysis calculated with different distribution functions and the composite function are plotted along with the results obtained with the dynamic-probabilistic model. It can be seen that with the exception of the Weibull function none of the frequency curves obtained by flood frequency analysis reflect the retention effect caused by dike breaches in contrast to the result of the dynamic-probabilistic model. For large and rare events the dynamic-probabilistic model predicts discharges asymptotically approaching maximum discharge. This discharge can be regarded as the probable maximum flood (PMF).

The Weibull function shows a similar characteristic as the derived flood frequency curve. However, the discharges predicted for extreme events are very low: Even for return intervals larger than 10000 years the discharge stays below the dike crests, i.e. no floodplain inundation will occur in this case. This means that the asymptotical behaviour of the frequency curve does not describe the actual peak attenuating process. On the contrary, in this case it rather shows the inappropriateness of the function despite the comparatively high likelihood weights (cf. Figure 9).

In order to test the plausibility of the model results, the model estimates for the 1000-year flood at the gauges Düsseldorf and Rees (downstream of Cologne) as well as the corresponding estimates on the basis of a flood frequency analysis with a log-normal distribution were compared with observed outstanding flood events in Germany and other European countries. The comparison is based on specific peak specific discharges (Figure 10-A). For this purpose the data base of Stanescu (2002) was extended by data from Herschy

(2003) and by various discharge data from the flood events that occurred recently, i.e. in 1997, 1999, 2002 and 2005, in Germany.

Figure 10-A illustrates that there is an upper bound of the specific discharge that declines with increasing catchment area. Both the model estimates and the estimates of the log-normal distribution exceed the specific flood discharges observed in Germany at comparable gauges. However, Figure 10-B illustrates that higher specific discharges occurred in other European catchments of a similar size (e.g. Danube, Don, Wisla, Odra). While the estimates of the dynamic-probabilistic model for the 1000-year flood at the gauges Düsseldorf and Rees are in the range of the observed specific discharges, the estimates of the log-normal distribution are the utmost margin of the data. This indicates that the dynamic-probabilistic model yields more realistic estimates of extreme flood discharges in comparison to a standard extreme value statistics approach.

5. Conclusion

The influence of dike breaches on the flood hazard situation along rivers with dikes that protect large former flood plains has not been systematically examined. Flood frequency analysis is usually not suited for such an analysis, since extreme events are not sufficiently represented in the data sample, or since the assumption of flood frequency analysis are violated. Therefore, a dynamic-probabilistic model has been developed that links simplified modules describing the processes of the river-dike-flood plain system within a Monte Carlo framework. In this way, it is possible to derive "process-oriented" flood frequency distributions.

The model is applied to the Lower Rhine in Germany. The results agree well with the usually used approach, i.e. the flood frequency approach, for flood events where no dike breaches occur. However, for extreme floods (e.g. 1000-year flood) dike breaches lead to large retention effects altering the flood frequency curve. The resulting probabilistic statements are

much more realistic than those of the flood frequency approach, since the dynamic-probabilistic model incorporates an important flood process that only occurs when a certain threshold is reached. Above this threshold the behaviour of the flood frequency curve is dominated by dike failures and floodplain inundation. The dynamic-probabilistic model acknowledges the fact that large floods are not large versions of small floods – an assumption that is implicitly built into flood frequency analysis.

The proposed method is principally transferable to any other diked river reach. However, the necessary preprocessing works are quite intensive in terms of data demand and computation time, while the actual model is very computational efficient. Therefore we recommend to use the model in another area for multiple purposes, e.g. the derivation of derived flood frequencies and risk assessments for different development scenarios, in order to optimise the benefits gained by the model.

References

Alkema, D. and Middelkoop, H., 2005. The influence of floodplain compartmentalization on flood risk within the Rhine-Meuse delta. Natural Hazards, 36(1-2)j 125-145.

Apel, H., Thieken, A.H., Merz, B. and Blöschl, G., 2004. Flood risk assessment and associated uncertainty. Natural Hazards and Earth System Science, 4(2): 295-308.

Apel, H., Thieken, A.H., Merz, B. and Blöschl, G., 2006. A Probabilistic Modelling System for Assessing Flood Risks. Natural Hazards, 38(1 - 2): 79-100.

Bates, P.D. and De Roo, A.P.J., 2000. A simple raster-based model for flood inundation simulation. Journal of Hydrology, 236(1-2): 54-77.

Brunner, G. W., 2002. HEC-RAS River Analysis System - Hydraulic Reference Manual. Davis. US Army Corps of Engineers - Hydrologic Engineering Center (HEC): 350 pp. (http://www.hec.usace.army.mil/software/hec-ras/documents/hydref/index.html)

Chbab, E.H., 1995. How extreme were the 1995 flood waves on the rivers Rhine and Meuse? Physics and Chemistry of the Earth, 20(5-6): 455-458.

Chow, V.T., 1973. Open-Channel Hydraulics, McGraw-Hill, 680 pp.

Disse, M. and Engel H., 2001. Flood events in the Rhine Basin: Genesis, Influences and Mitigation. Natural Hazards, 23: 271-290.

Engel, H., 2004. The flood event 2002 in the Elbe river basin: causes of the flood, its course, statistical assessment and flood damages. Houille-Blanche, (6): 33-36.

EU, 2006. http://ec.europa.eu/environment/water/flood_risk/index.htm

Fink, A., Ulbrich, U. and Engel, H., 1996. Aspects of the January 1995 flood in Germany. Weather 51(2): 34-39.

Gutknecht, D., 1994. Extremhochwässer in kleinen Einzugsgebieten. Österreichische Wasser- und Abfallwirtschaft, 46(3/4), 50-57.

Helms, M., Büchele, B., Merkel, U. and Ihringer, J., 2002. Statistical analysis of the flood situation and assessment of the impact of diking measures along the Elbe (Labe) river. Journal of Hydrology, 267(1-2), 94-114.

Herschy, R., 2003: World catalogue of maximum observed floods. IAHS Publication 284: 285 pp.

Hewlett, H. W. Boorman, M., L. A. and Bramley, M. E., 1987. Design of reinforced grass waterways (CIRIA Report 116). London, Construction Industry Research and Information Association (CIRIA), 118 pp.

Hosking, J.R.M. and Wallis, J.R., 1997. Regional Frequency Analysis, An Approach Based on L-Moments. Cambridge University Press, Cambridge, 240 pp.

Hunter, N.M., Horritt, M., Bates, P.D., Wilson, M.D. and Werner, M.G.F., 2005. An adaptive time step solution for raster-based storage cell modelling of floodplain inundation. Advances in Water Resources, 28(9): 975-991.

ICPR (International Commission for the Protection of the Rhine), 2001. Rhine-Atlas. ICPR, Koblenz, retrieved from http://www.rheinatlas.de (11 October 2006).

Jain, S. and Lall, U., 2001. Floods in a changing climate; does the past represent the future? Water Resources Research, 37(12), 3193-3205.

Jothityangkoon, C. and Sivapalan, M., 2003. Towards estimation of extreme floods; examination of the roles of runoff process changes and floodplain flows. Journal of Hydrology, 281(3): 206-229.

Kamrath, P., Disse, M., Hammer, M. and Köngeter, J., 2006. Assessment of discharge through a dike breach and simulation of flood wave propagation. Natural Hazards, 38(1-2), 63-78.

Kortenhaus, A. and Oumeraci, H., 2002. Probabilistische Bemessungsmethoden für Seedeiche (ProDeich). Bericht No. 877, Leichtweiss-Institut, Braunschweig, pp. 205.

Lammersen, R., Engel, H., Van de Langemheen, W. and Buiteveld, H., 2002. Impact of river training and retention measures on flood peaks along the Rhine. Journal of Hydrology, 267(1-2), 115-124.

Merz, B., Apel, H., Gocht, M., 2004. Entwicklung eines probabilistischen Ansatzes zur Bestimmung des Deichversagens durch Überströmen. In: Merz, B., Apel, H. (eds.), Risiken durch Naturgefahren, Scientific Technical Report STR04/01, GeoForschungsZentrum Potsdam, 77-84.

Milly, P.C.D., Wetherald, R.T., Dunne, K.A. and Delworth, T.L., 2002. Increasing risk of great floods in a changing climate. Nature, 415(6871), 514-517.

MURL, 2000. Potentielle Hochwasserschäden am Rhein in NRW. Ministry of Environment. Spatial Planning and Agriculture of North Rhine-Westphalia. Düsseldorf. retrieved from http://www.proaqua-gmbh.de/hws/hwsnrw/hws/index.htm (11 October 2006)

Stanescu, V.A., 2002. Outstanding floods in Europe: A regionalization and comparison. In: International Conference on Flood Estimation, Berne, Switzerland CHR-Report II-17,

Stedinger, J.R., Vogel, R.M. and Foufoula-Georgiou, E., 1993. Frequency analysis of extreme events. In: D.R. Maidment (Editor), Handbook of Hydrology. McGraw-Hill, New York, pp. 18.1 - 18.66.

USACE, 1999. Risk-based analysis in geotechnical engineering for support of planning studies. Engineer Technical Letter (ETL) 1110-2-556, U.S. Army Corps of Engineers, Washington D.C.

Vrijling, J.K., 2000. Probabilistic Design. Lecture Notes, pp. 145, Delft.

Werner, M.G.F., Hunter, N.M. and Bates, P.D., 2005. Identifiability of distributed floodplain roughness values in flood extent estimation. Journal of Hydrology, 314(1-4): 139-157.

Wind, H.G, Nierop, T.M., de Blois, C.J. and de Kok, J.L., 1999. Analysis of flood damages from the 1993 and 1995 Meuse flood. Water Resources Research, 35(11): 3459-3465.

Woltemade, C.J. and Potter, K.W., 1994. A watershed modeling analysis of fluvial geomorphologic influences on flood peak attenuation. Water Resources Research, 30(6): 1933-1942.

Wood, E.F. and Rodriguez-Iturbe, I., 1975. A bayesian approach to analyzing uncertainty among flood frequency analysis. Water Resources Research, 11(6): 839-843.

Figure captions:

Figure 1: The investigation area Lower Rhine between Cologne and Rees.

Figure 2: Fit of five different extreme value distributions to the annual maximum discharge series of Cologne from 1961-1995 and the composite distribution function constructed by the likelihood weights given for each function in the legend.

Figure 3: Superposition of the synthetic flood waves of the Rhine and the tributaries Ruhr and Lippe for each flood type identified in the cluster analysis. The flood waves are scaled in time, but normalised in flood peaks to show the delay of flood peaks. P indicates the probability of a flood to belong to the respective clusters.

Figure 4: Flood wave attenuation and translation for the flood event of 1993 in the study reach.

Figure 5: Fit of the empirical formula for the critical dike overflow velocity (3) to experimental data published by Hewlett et al. (1987), Goodness if fit: RMSE = 0.06844 m/s, coefficient of determination $R^2 = 0.954$.

Figure 6: Conditional failure probabilities (fragility surface) for breach location 1 depending on overflowing duration and overtopping height.

Figure 7: Scheme of the dynamic-probabilistic model for a single Monte-Carlo run.

Figure 8: Plot of discharges for selected return intervals along the river reach. The solid lines represent the results of the dynamic-probabilistic model, the markers the results of extreme value analysis (composite function) for the gauging stations.

Figure 9: Comparison of extreme value statistics for the gauging stations Düsseldorf, Ruhrort and Rees with the result of the dynamic-probabilistic model. The numbers in the legend give the likelihood weights associated to the five basic distributions, which were use for the construction of the composite function.

Figure 10: Comparison of estimates for the 1000-year flood at the gauges Düsseldorf and Rees with observed outstanding flood events in Germany and other European countries (data from Stanescu, 2002, Herschy, 2003 and various gauging stations in Germany).
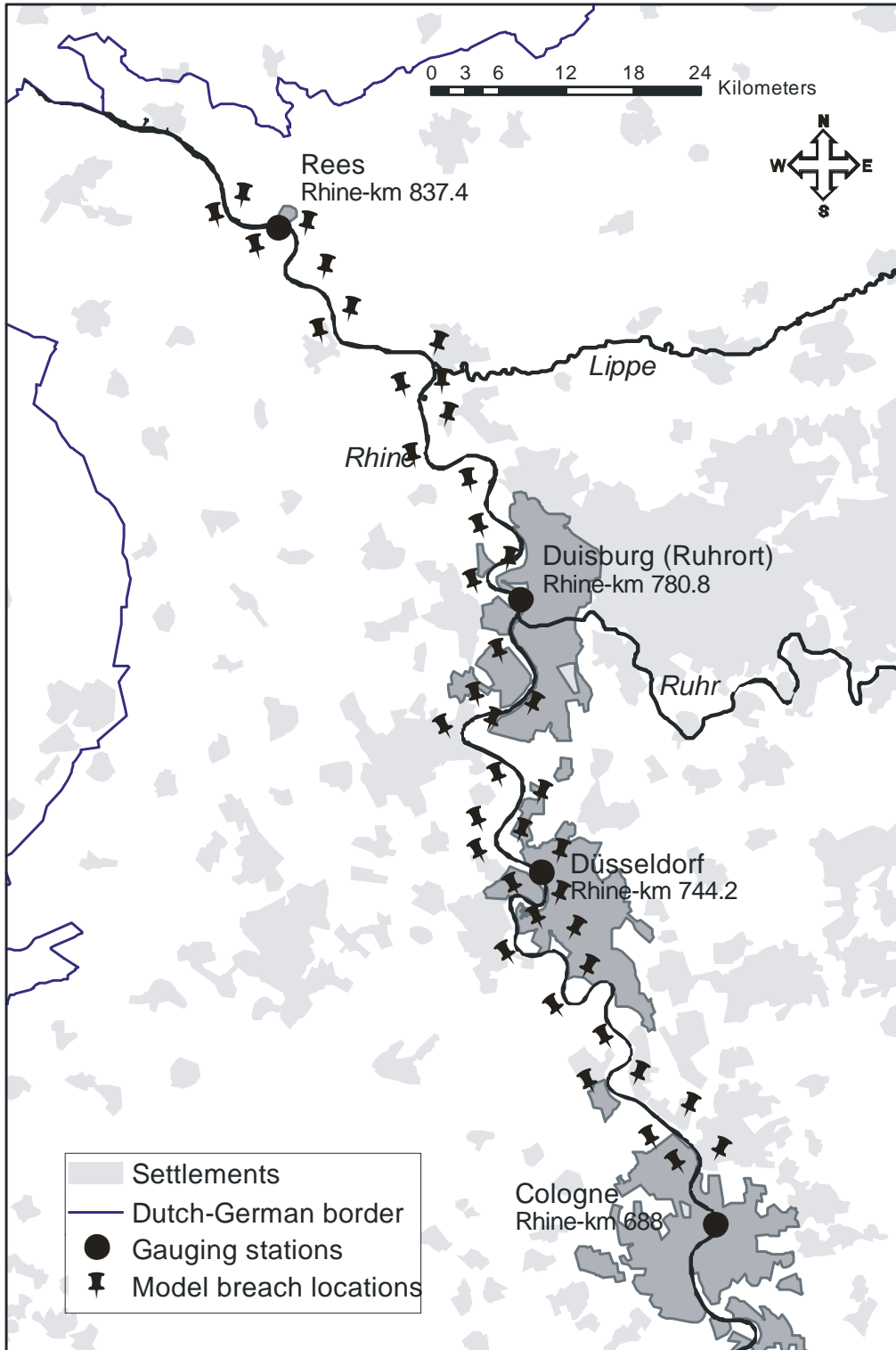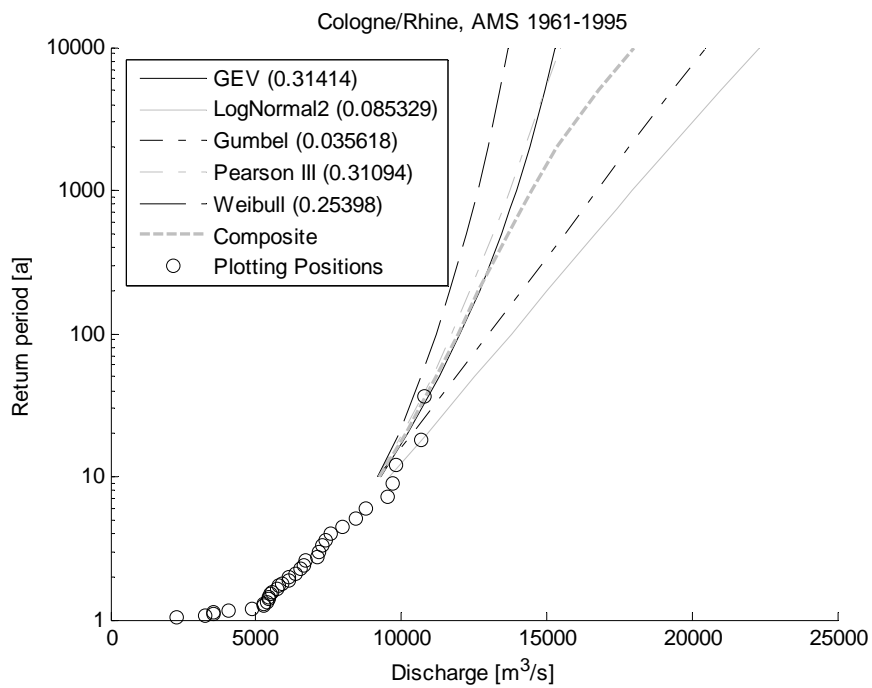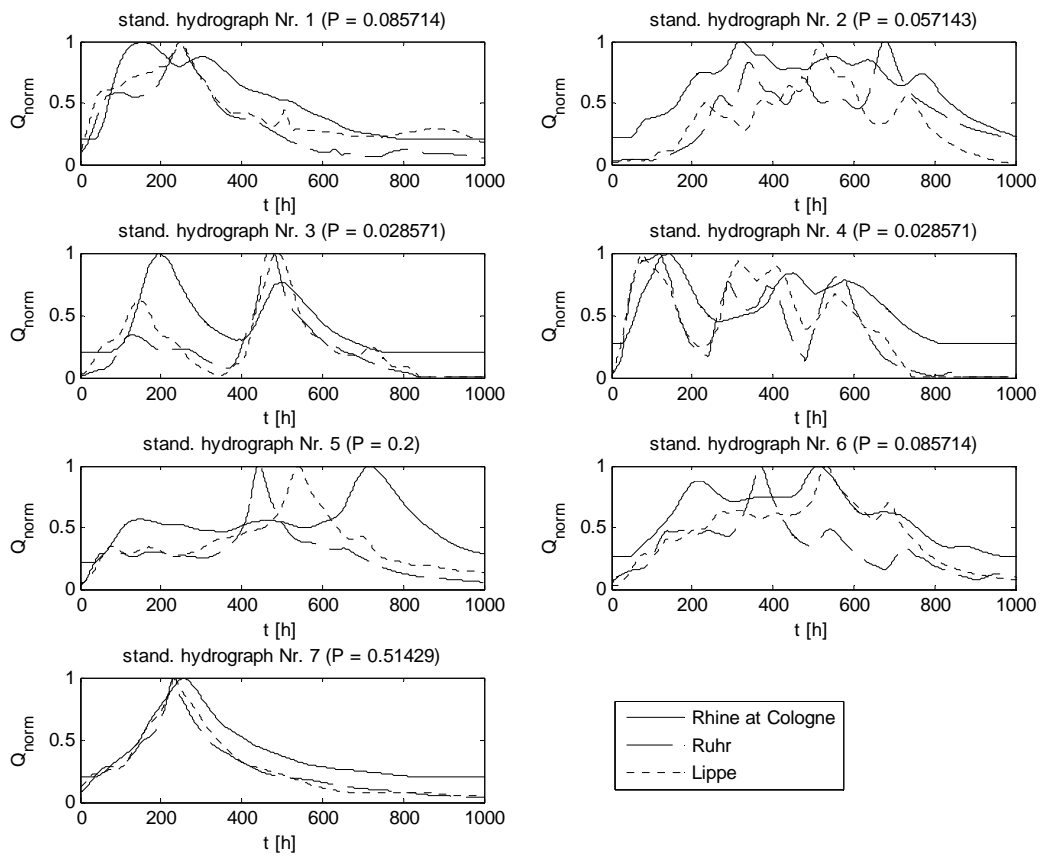
Figure 1

Figure 2

Cologne/Rhine, AMS 1961-1995

Figure 3

stand. hydrograph Nr. 1 (P = 0.085714)

stand. hydrograph Nr. 2 (P = 0.057143)

stand. hydrograph Nr. 3 (P = 0.028571)

stand. hydrograph Nr. 4 (P = 0.028571)

stand. hydrograph Nr. 5 (P = 0.2)

stand. hydrograph Nr. 6 (P = 0.085714)

stand. hydrograph Nr. 7 (P = 0.51429)
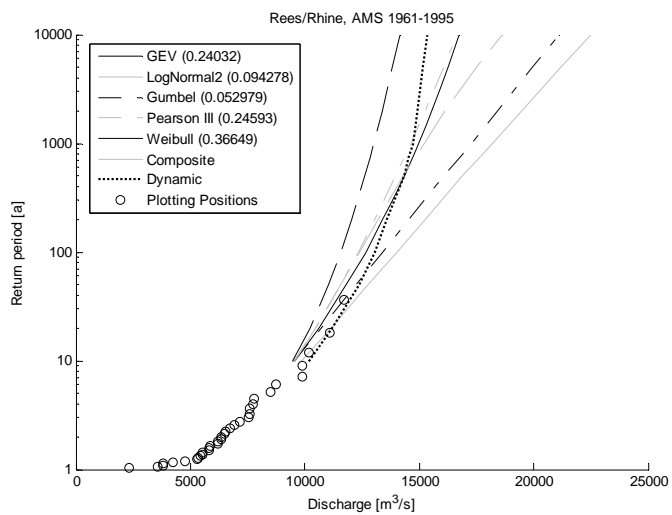
Rhine at Cologne
Ruhr
Lippe
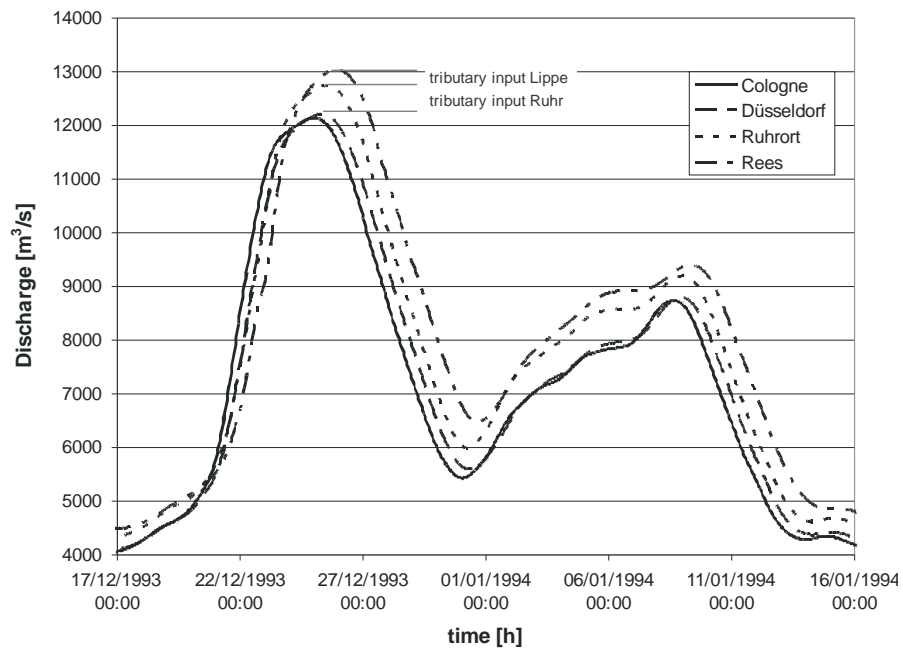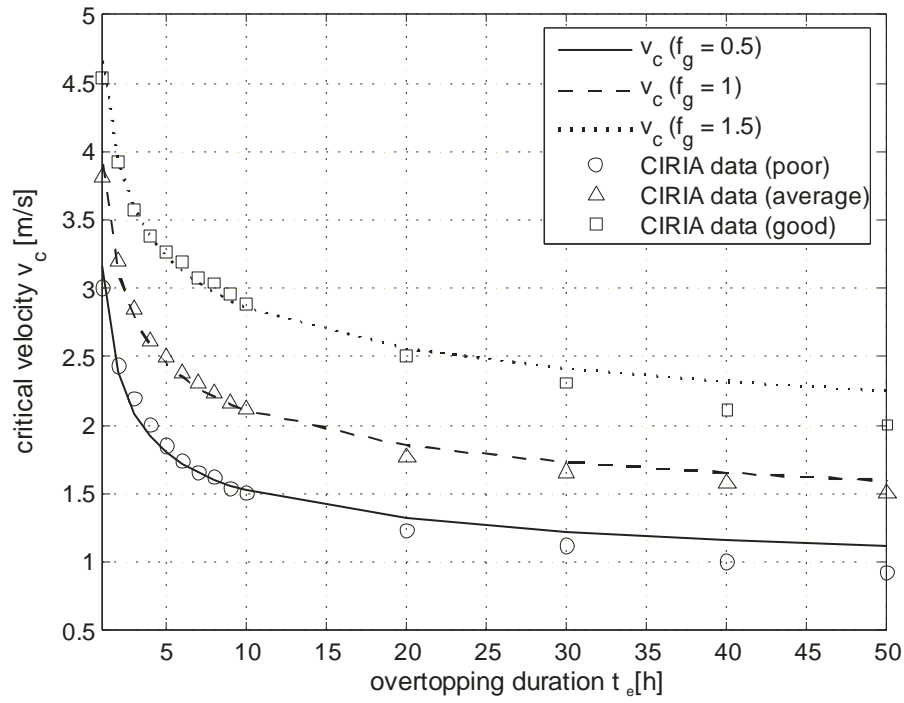
Figure 4

Figure 5

Figure 6
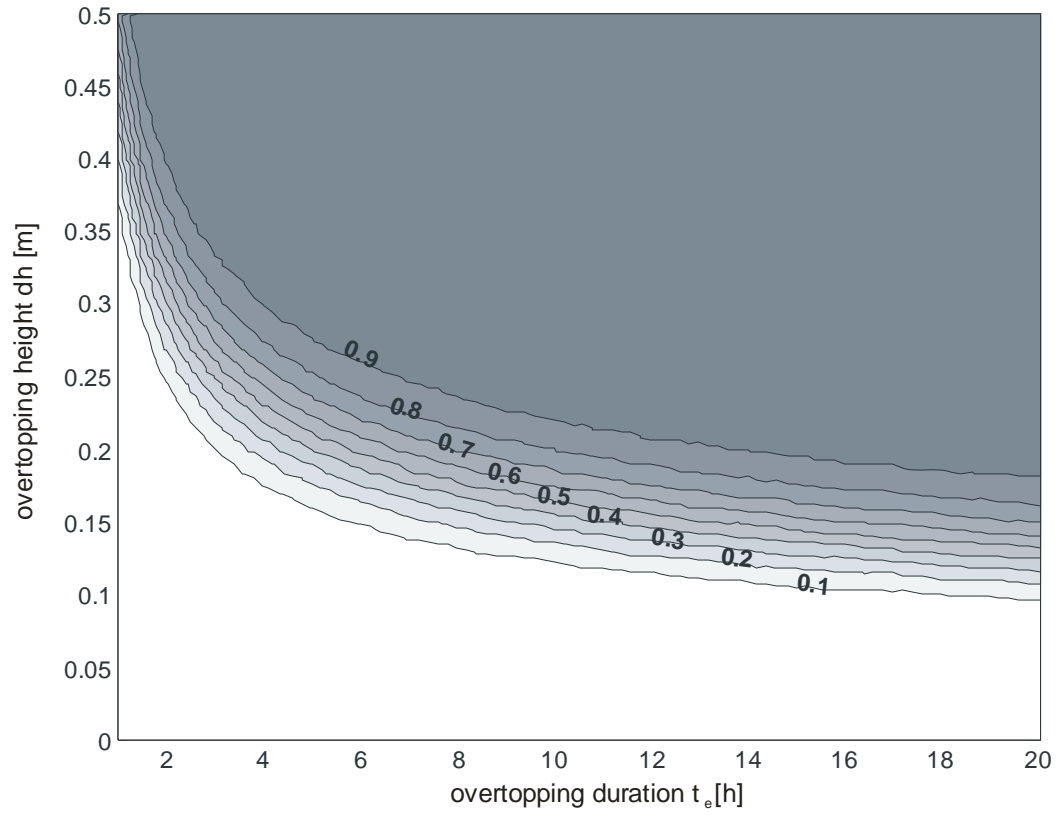
Figure 7
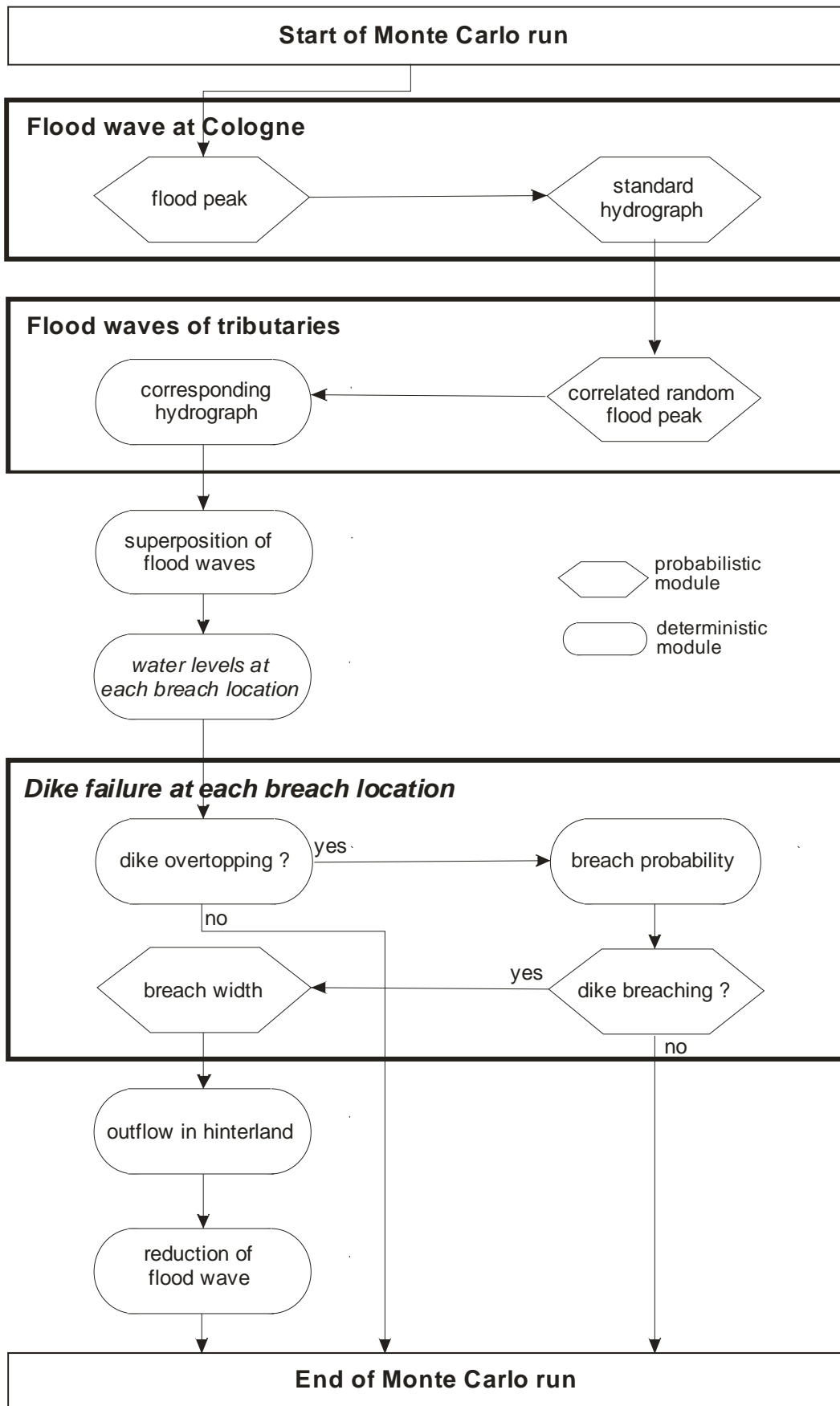
Figure 8

Figure 9

Figure 10